

## Seeing Molecules Interact with Total Internal Reflection Fluorescence Microscopy

See-Lok Ho, Hung-Wing Li and Man Shing Wong\*

Department of Chemistry, Hong Kong Baptist University, Hong Kong

\*Corresponding author: Hung-Wing Li and Man Shing Wong, Department of Chemistry, Hong Kong Baptist University, Hong Kong, E-mail: [hwli@hkbu.edu.hk](mailto:hwli@hkbu.edu.hk), [mshwong@hkbu.edu.hk](mailto:mshwong@hkbu.edu.hk)

Received date: 21 Dec 2015; Accepted date: 16 Feb 2016; Published date: 20 Feb 2016.

Citation: Ho LS, Li WH, Wong MS (2016) Seeing Molecules Interact with Total Internal Reflection Fluorescence Microscopy. J Biochem Analyt Stud 1(1): doi <http://dx.doi.org/10.16966/2576-5833.102>

Copyright: © 2016 Ho LS, et al. This is an open-access article distributed under the terms of the Creative Commons Attribution License, which permits unrestricted use, distribution, and reproduction in any medium, provided the original author and source are credited.

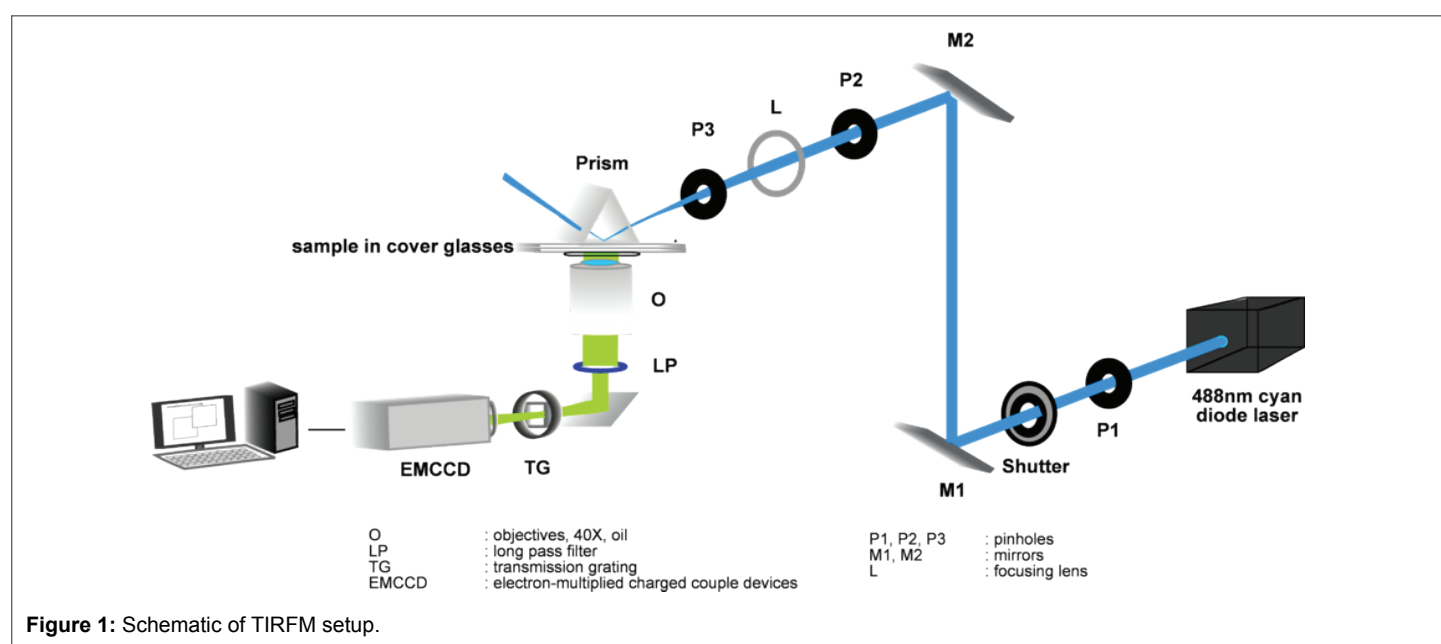
Fluorescence microscopy has been widely applied in many different biological aspects for sensing and imaging of biological samples, including cell imaging, real time monitoring of biomolecules and biomarkers detection. The commonly utilized light microscopy techniques are confocal, epi-fluorescence, multi-photon, total internal reflection fluorescence microscopy (TIRFM). Amongst all the fluorescence imaging techniques, TIRFM, also known as the evanescent field microscopy, has received considerable attention due to its unique properties. TIRFM is considered as a powerful technique, which enable *in-vivo* and *in-vitro* monitoring of dynamic and kinetic interaction of the biomolecules in single-molecules and single-cells level.

### Configuration and Properties of TIRFM

Total internal reflection occurs when the excitation light beam propagating through a dense medium (high refractive index) encounter another less dense medium (low refractive index) with an incident angle greater than the critical angle ( $\theta_c$ ). The critical angle is derived by Snell's law:  $\theta_c = \sin^{-1}(n_2/n_1)$ , where  $n_2$  and  $n_1$  are the refractive index of the dense and less dense medium respectively. Instead of propagated through the less dense medium, certain amount of incident light is reflected off at the interface, this phenomenon is known as total internal reflection. At the same time, some of the incident energy will transmit through the

interface and generated a standing electromagnetic field called evanescent field. Unlike other form of light, evanescent light decays in the intensity exponentially over a sub-wavelength distance. The intensity of the evanescent field ( $I_z$ ) at any position ( $z$ ) can be calculated by  $I_z = I_0 \exp^{-z/d}$ , where  $I_0$  is the intensity at  $z=0$ ,  $d$  is the penetration depth of the evanescent field that can be obtained by  $d = \lambda / (4\pi (n_1^2 \sin^2 \theta - n_2^2)^{1/2})$ , where  $\lambda$  is the wavelength of the excitation light beam in vacuum. The penetration depth of the light beam is typically ~100-300 nm. In a prism-type TIRFM the penetration depth can be controlled by three factors: (i) the wavelength of the excitation source, the longer the wavelength of the light source, the deeper the evanescent field is. (ii) The incident angle of the light source, the penetration depth decreases while increasing the incident angle. The last but not least, (iii) refractive index of the less dense medium, as the refractive index of the less dense medium increases, the penetration depth also increases.

In TIRFM since the intensity of the evanescent field decays exponentially, fluorophores closer will be excited more strongly than the fluorophores away from the interface, which gives a high-contrast image of the fluorophores near the interface. In addition, because of the penetration depth of the evanescent field is very shallow, only fluorophores within the field will be excited, while the rest in the bulk solution will remain "silent". It gives a high signal-to-noise ratio and reduces the photo-damage on the analytes.



## Real-Time Monitoring of Single Biomolecules and Cells

Reports have demonstrated the capability of TIRFM for *in-vitro* quantification of disease associated biomarkers for instances, a single-molecule detection assay for quantification of microRNAs (miRNAs) and circulating miRNAs in cell lysate and human serum samples. The developed assays are highly sensitive, specific, and successively differentiate different stages of cancer [1,2]. Researchers also applied TIRFM imaging system to monitor the aggregation kinetics of beta-amyloid peptide [3-10]. Simon group reported the utility of TIRFM as one of the imaging approaches to reveal a previously unobserved view of the genesis of individual virions. They were also able to explore the different parameters of viral assembly that are inaccessible with other conventional techniques [11]. Nosrati et al. [12] monitored the sperm motion which is well-known to be a crucial role in fertilization and were able to resolve the nature of this motion. Using TIRFM, they selectively imaged motile human and bull sperm to revealing a two-dimensional (2D) 'slither' swimming mode. This behavior was found to be distinguishable from bulk and near-wall swimming modes. The influence of media viscosity was studied and a strategy was suggested for the human sperm that is suitable for the highly viscous and confined lumen within the fallopian tube [12]. Real-time monitoring and tracking of single molecules or single cells in wide field mode is very attractive for high-throughput studies. Coupling several lasers of different excitation wavelengths which can be switched in microseconds precisely with an acousto-optical tunable filter (AOTF) allows sophisticated multi-color biomolecular imaging and tracking [13].

TIRFM is no longer limited to 2D imaging; Fang group demonstrated that the z-positions of fluorescent nano particles close to the cell basal lateral membrane can be extracted by collecting the fluorescence intensities at different incident angles. Once the incident angle is reduced to be in the sub-critical range, the TIRFM works as a pseudo-TIRFM by which the whole cell-body can be monitored from bottom to top [14]. Three-dimensional tracking strategies are hence established [13].

In short, highly sensitive single-molecules and single-cells fluorescence microscopy techniques, like TIRFM, are powerful tools for addressing clinical and scientific challenges. However, novel with high spatial resolution microscopy techniques are valuable tools to evaluate the functionality of those interested biomolecules in a complex cellular environment.

## References

- Chan HM, Chan LS, Wong RNS, Li HW (2010) Direct Quantification of Single-Molecules of MicroRNA by Total Internal Reflection Fluorescence Microscopy. *Anal Chem* 82: 6911-6918.
- Ho SL, Chan HM, Ha AWY, Wong RNS, Li HW (2014) Direct Quantification of Circulating MiRNAs in Different Stages of Nasopharyngeal Cancerous Serum Samples in Single Molecule Level with Total Internal Reflection Fluorescence Microscopy. *Anal Chem* 86: 9880-9886.
- Chan HM, Xiao LH, Yeung KM, Ho SL, Zhao D, et al. (2012) Li H W Effect of surface-functionalized nanoparticles on the elongation phase of beta-amyloid (1-40) fibrillogenesis. *Biomaterials* 33: 4443-4450.
- Ho SL, Poon CY, Lin C, Yan T, Kwong DW, et al. (2015) Inhibition of beta-Amyloid Aggregation by Albiflorin Aloeemodin and Neohesperidin and their Neuroprotective Effect on Primary Hippocampal Cells Against beta-Amyloid Induced Toxicity. *Curr Alzheimer Res* 12: 424-433.
- Xiao LH, Zhao D, Chan WH, Choi MM, Li HW (2010) Inhibition of beta 1-40 amyloid fibrillation by N-acetylcysteine-capped quantum dots. *Biomaterials* 31: 91-98.
- Lu L, Zhong HJ, Wang M, Ho SL, Li HW, et al. (2015) Inhibition of Beta-Amyloid Fibrillation by Luminescent Iridium(III) Complex Probes. *Sci Rep* 5.
- Man BYW, Chan HM, Leung CH, Chan DSH, Bai LP, et al. (2011) Group 9 metal-based inhibitors of beta-amyloid (1-40) fibrillation as potential therapeutic agents for Alzheimer's disease. *Chem Sci* 2: 917-921.
- Ng OTW, Wong Y, Chan H M, Cheng J, Qi X, et al. (2013) N-Acetyl-L-cysteine capped quantum dots offer neuronal cell protection by inhibiting beta (1-40) amyloid fibrillation. *Biomater Sci* 1: 577-580.
- Xiao LH, Zhao D, Chan WH, Choi MM, Li HW, et al. (2010) Inhibition of beta 1-40 amyloid fibrillation with N-acetyl-L-cysteine capped quantum dots. *Biomaterials* 31: 91-98.
- Yang WG, Wong Y, Ng OTW, Bai LP, Kwong DWJ, et al. (2012) Inhibition of Beta-Amyloid Peptide Aggregation by Multifunctional Carbazole-Based Fluorophores. *Angew Chem Int Ed Engl* 51: 1804-1810.
- Jouvenet N, Bieniasz PD, Simon SM (2008) Imaging the biogenesis of individual HIV-1 virions in live cells. *Nature* 454: 236-240.
- Nosrati R, Driouchi A, Yip C M, Sinton D (2015) Two-dimensional slither swimming of sperm within a micrometre of a surface. *Nat Commun* 6.
- Ruthardt N, Lamb DC, Brauchle C (2011) Single-particle Tracking as a Quantitative Microscopy-based Approach to Unravel Cell Entry Mechanisms of Viruses and Pharmaceutical Nanoparticles. *Mol Ther* 19: 1199-1211.
- Sun W, Xu AS, Marchuk K, Wang GF, Fang N (2011) Whole-Cell Scan Using Automatic Variable-Angle and Variable-Illumination-Depth Pseudo-Total Internal Reflection Fluorescence Microscopy. *J Lab Autom* 16: 255-262.